Available online at www.sciencedirect.com
ScienceDirect
Journal of Sound and Vibration 297 (2006) 457–476
JOURNAL OF SOUND AND VIBRATION
www.elsevier.com/locate/jsvi

Buckling and vibration of polar orthotropic circular plate resting on Winkler foundation

U.S. Gupta*, A.H. Ansari, S. Sharma

Department of Mathematics, Indian Institute of Technology Roorkee, Roorkee-247667, India

Received 13 July 2004; received in revised form 20 September 2005; accepted 31 January 2006
Available online 10 July 2006

Abstract

Buckling and vibrational behavior of polar orthotropic circular plates of linearly varying thickness is presented on the basis of classical plate theory. The plate is resting on Winkler-type foundation. An approximate solution has been obtained by Ritz method, which employs basis functions based upon static deflection of polar orthotropic plates. The effect of elastic foundation and that of orthotropy on the natural frequency of plate has been illustrated for different values of taper parameter, flexibility parameter, in-plane force and nodal diameter. The critical buckling load for clamped and simply supported plates have been obtained. A comparison of results with those available in literature has been presented.

1. Introduction

The increasing use of orthotropic materials in modern aerospace structures has necessitated the study of vibrational characteristics of plate-type components fabricated by these materials. Circular and annular plates are extensively used as structural components for diaphragms and deckplates in launch vehicles. The consideration of thickness variation together with anisotropy not only reduces the size and weight of components, but also meets the desirability of high strength, corrosion resistance and high-temperature performance.

A considerable amount of work dealing with vibration of polar orthotropic circular/annular plates of uniform/non-uniform thickness is available in literature and few of them are reported in Refs. [1–11]. The problem of plates resting on an elastic foundation finds application in foundation engineering such as reinforced concrete pavements of high runways, foundation of deep wells, storage tanks and slabs of buildings(Szilard [12, p. 136]). Various models such as Winkler (Chonan [13], Gupta et al. [14] and Liew et al. [15]), Pasternak (Wang and Stephans [16]) and Vlasov (Bhattacharya [17]) have been proposed in the literature.

*Corresponding author.
E-mail address: usgptfma@iitr.ernet.in (U.S. Gupta).

0022-460X/$ - see front matter
doi:10.1016/j.jsv.2006.01.073

Nomenclature

r,θ	polar coordinates of a point in the mid-plane of the plate
a	radius of the circular plate
R	r/a, non-dimensional radius vector
t	time
W	$W(r,\theta,\ t)$ transverse displacement function
W_i	shape function
$E_r,\ E_\theta$	Young's moduli of elasticity along r and θ directions, respectively
$G_{r\theta}$	shear modulus
$v_r,\ v_\theta$	Poisson's ratio defined as a strain in tangential and radial directions, respectively.
h_0	non-dimensional thickness of the plate at the center
h	$h(r)$, thickness of the plate
α	taper parameter
α_i,β_i	constants
$A_i,\ C_i$	constants
$D_r,\ D_\theta$	$E_r h^3/12\ (1-v_r v_\theta)$, $E_\theta h^3/12\ (1-v_r v_\theta)$ flexural rigidities along r and θ directions, respectively.
D_{r0}	$E_r h_0^3/12(1-v_r v_\theta)$
$D_{r\Theta}$	$G_{r\theta} h^3/12$ shear rigidity
D_k	$4D_{r\theta}$
D_{k0}	D_k/D_{r0}
$N_r,\ N_\theta$	radial and circumferential stress resultants in the plate
k_Φ	stiffness of the spring against rotation
K_Φ	foundation modulus
k_f	$a^4 k_f\ (/D_{\mathrm{r0}}$
n	nodal diameter
N	in plane force
$\bar{N}$	Na^2/D_{r0}
p^2	E_θ/E_r, rigidity ratio
ρ	density of the plate material
ω	circular frequency in rad/s
Ω^2	$a^4\rho\omega^{\mathrm{I}} h_0/D_{r0}$ frequency parameter
λ	$1-p$

In various engineering applications, plates are often subjected to in-plane stressing due to compressive loads which may induce buckling, a phenomenon which is highly undesirable. This consideration is important for the design of structural components. Thus, the study of stability of plates assumes great significance. Keeping this in view Gupta et al. [18] analyzed the combined effect of axial force and elastic foundation of polar orthotropic annular plates using quintic splines technique.

Various numerical methods such as finite difference (Greenberg and stavsky [19]) and finite elements (Chen and Ren [20], Liu and Lee [21], Charbonneau [22]) require fine mesh size to obtain accurate results but are computationally expensive. Ritz method is one of the most popular methods for obtaining approximate solutions for frequencies and modes of vibration of elastic plates. It was applied by its inventor to study free vibration of a plate a century ago in 1909 [23]. Ritz method has the advantage of high accuracy and computational efficiency which greatly depends upon the choice of admissible functions. The method has also been used for thick plates [24] with different geometries. Bhat [25,26] introduced the use of characteristic orthogonal polynomials in Rayleigh–Ritz method in the study of flexural vibration of rectangular and polygonal plates. Dickinson and Blasio [27] modified the set of orthogonal polynomials to study vibration and buckling of orthotropic rectangular plates. Liew et al. [28,29] and Liew and Lam [30] proposed a set of two-dimensional plate functions generated by using Gram–Schmidt process in analyzing flexural vibration of triangular, rectangular and skew plates of uniform thickness in employing Rayleigh–Ritz method. Liew [31] applied the so-called pb-2 Ritz method to study free flexural vibrations of symmetrically laminated circular plates. Recently, Zhou et al. [32] used Ritz method for three-dimensional vibration analysis of thick rectangular plates while Zhou et al. [33] applied it to the study of circular and annular plates. Kang [34] used Ritz method for vibration analysis of circular and annular plates with nonlinear thickness variation. Kang et al. [35] applied Rayleigh–Ritz method for free vibration analysis of polar orthotropic circular plates.

In the present paper, the effect of elastic foundation on vibrations and buckling of polar orthotropic circular plates of linearly varying thickness with elastically restrained edge has been analyzed by Ritz method. A new type of basis functions based upon static deflection of polar orthotropic plates given by Lekhnitskii [36] have been chosen which leads to faster rate of convergence as compared to the choice of polynomial coordinate functions used in Ref. [37].

2. Analysis

Consider a thin circular plate of radius a, variable thickness $h = h(r)$, resting on elastic foundation of modulus k_f, elastically restrained against rotation by springs of stiffness k_Φ and subjected to hydrostatic in-plane force N at the periphery. Let (r,θ) be the polar coordinates of any point on the neutral surface of the circular plate shown in Fig. 1.

The maximum kinetic energy of the plate is given by

$$T_{\max} = \frac{1}{2}\rho\omega^2 \int_0^a \int_0^{2\pi} hW^2 r \,\mathrm{d}\theta \,\mathrm{d}r, \tag{1}$$

where W is the transverse deflection, ρ the mass density and ω the frequency in rad/s.

The maximum strain energy of the plate is given by

$$\begin{aligned} U_{\max} = \frac{1}{2}\int_0^a \int_0^{2\pi} \Bigg[& D_r \left\{ \left(\frac{\partial^2 W}{\partial r^2}\right)^2 + 2\upsilon_\theta \frac{\partial^2 W}{\partial r^2}\left(\frac{1}{r}\frac{\partial W}{\partial r} + \frac{1}{r^2}\frac{\partial^2 W}{\partial \theta^2}\right)\right\} \\ & + D_\theta \left(\frac{1}{r}\frac{\partial W}{\partial r} + \frac{1}{r^2}\frac{\partial^2 W}{\partial \theta^2}\right)^2 + D_k \left\{ \frac{\partial}{\partial r}\left(\frac{1}{r}\frac{\partial W}{\partial \theta}\right)\right\}^2 \\ & + k_f W^2 + N_r \left(\frac{\partial W}{\partial r}\right)^2 + N_\theta \left(\frac{1}{r}\frac{\partial W}{\partial \theta}\right)^2 \Bigg] \\ & \times r \,\mathrm{d}\theta \,\mathrm{d}r + \frac{1}{2} a k_\phi \int_0^{2\pi} \left(\frac{\partial W(a,\theta)}{\partial r}\right)^2 \mathrm{d}\theta, \end{aligned} \tag{2}$$

where $1/k_\Phi$ is the rotational flexibility of the spring and k_f the foundation modulus:

$$D_r = \frac{E_r h^3}{12(1-\upsilon_r\upsilon_\theta)}, \quad D_\theta = \frac{E_\theta h^3}{12(1-\upsilon_r\upsilon_\theta)}, \quad D_k = \frac{G_{r\theta} h^3}{3}$$

are flexural rigidities of the plate and N_r and N_θ are the radial and circumferential stress resultants.

The stress equilibrium equation of the plate in radial direction is given by

$$r\frac{\partial N_r}{\partial r} + N_r - N_\theta = 0. \tag{3}$$

The compatibility equation of the plate is given by

$$r\frac{\partial \varepsilon_\theta}{\partial r} + \varepsilon_\theta - \varepsilon_r = 0. \tag{4}$$

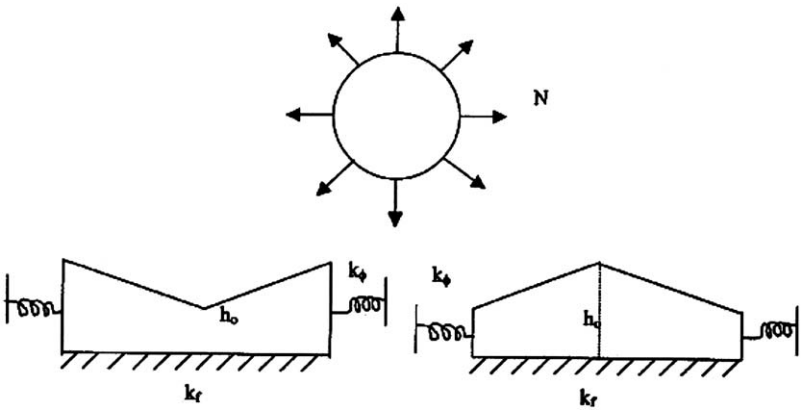

Fig. 1.

For polar orthotropic material, stress resultant–strain relationship is given by Lekhnitskii [37, p. 99]:

$$N_r = \frac{E_r}{(1-\upsilon_r\upsilon_\theta)}(\varepsilon_r + \upsilon_\theta\varepsilon_\theta),$$
$$N_\theta = \frac{E_\theta}{(1-\upsilon_r\upsilon_\theta)}(\varepsilon_\theta + \upsilon_r\varepsilon_r). \tag{5}$$

Introducing the non-dimensional variable $R = r/a$ and using the compatibility Eq. (4) for linearly varying thickness $h = h_0(1-\alpha R)$, the stress equilibrium Eq. (3) becomes

$$R^2\frac{d^2N_r}{dR^2} + \frac{(3-2\alpha R)}{(1-\alpha R)}R\frac{dN_r}{dR} + \left((1-p^2) - \frac{(1-\upsilon_\theta)\alpha R}{(1-\alpha R)}\right)N_r = 0, \tag{6}$$

where h_0 is the thickness of the plate at the center and α the taper parameter.

The solution of N_r obtained by Frobenius method [7] is given by

$$N_r = \frac{N}{1+\sum_1^\infty C_i}R^\lambda\left(1+\sum_1^\infty C_iR^i\right), \tag{7}$$

where

$$p = \sqrt{E_\theta/E_r},\ \lambda = 1-p, C_0 = 1 \quad \text{and}$$

$$C_i = \frac{(\lambda+i-1)(\lambda+i+1)+1-p^2-(\lambda+i-\upsilon_\theta)}{(\lambda+i+1)^2-p^2}\alpha C_{i-1}, \quad i = 1,2,3,\ldots,\infty.$$

3. Method of solution: Ritz method

Ritz method requires that the functional

$$J(W) = U_{\max} - T_{\max} = \frac{1}{2}\int_0^a\int_0^{2\pi}\left[D_r\left\{\left(\frac{\partial^2W}{\partial r^2}\right)^2 + 2\upsilon_\theta\frac{\partial^2W}{\partial r^2}\left(\frac{1}{r}\frac{\partial W}{\partial r}+\frac{1}{r^2}\frac{\partial^2W}{\partial\theta^2}\right)\right\}\right.$$
$$+ D_\theta\left(\frac{1}{r}\frac{\partial W}{\partial r}+\frac{1}{r^2}\frac{\partial^2W}{\partial\theta^2}\right)^2 + D_k\left\{\frac{\partial}{\partial r}\left(\frac{1}{r}\frac{\partial W}{\partial\theta}\right)\right\}^2 + k_fW^2 + N_r\left(\frac{\partial W}{\partial r}\right)^2 + N_\theta\left(\frac{1}{r}\frac{\partial W}{\partial\theta}\right)^2\Bigg]r\,d\theta\,dr$$
$$+\frac{1}{2}ak_\phi\int_0^{2\pi}\left(\frac{\partial W(a,\theta)}{\partial r}\right)^2 d\theta - \frac{1}{2}\rho\omega^2\int_0^a\int_0^{2\pi}hW^2r\,d\theta\,dr \tag{8}$$

be minimized.

Assuming the deflection function as

$$\overline{W} = \cos n\theta\sum_{i=0}^m A_iW_i(R) = \cos n\theta\sum_{i=0}^m A_i(1+\alpha_iR^4+\beta_iR^{1+p})R^{2i+n}, \tag{9}$$

where A_i are undetermined coefficients, $\bar{W} = W/a$ and α_i, β_i are unknown constants to be determined from boundary conditions (Leissa [1, p. 14])

$$K_\phi\frac{dW_i(1)}{dR} = -(1-\alpha)^3\left[\frac{d^2W_i}{dR^2}+\upsilon_\theta\left(\frac{1}{R}\frac{dW_i}{dR}-n^2\frac{W_i}{R^2}\right)\right]_{R=1}, \tag{10}$$

$$W_i(1) = 0. \tag{11}$$

Using non-dimensional variables $\overline{W}$ and R along with relation (9) the functional $J(W)$ given by (8) becomes

$$J = \frac{D_{r_0}}{2}\left[\int_0^1\int_0^{2\pi}\left[(1-\alpha R)^3\left\{\left(\frac{\partial^2\overline{W}}{\partial R^2}\right)^2 + 2\upsilon_\theta\,\frac{\partial^2\overline{W}}{\partial R^2}\left(\frac{1}{R}\frac{\partial\overline{W}}{\partial R}+\frac{1}{R^2}\frac{\partial^2\overline{W}}{\partial\theta^2}\right)\right.\right.\right.$$
$$\left.\left.+\,p^2\left(\frac{1}{R}\frac{\partial\overline{W}}{\partial R}+\frac{1}{R^2}\frac{\partial^2\overline{W}}{\partial\theta^2}\right)^2\right\} + D_{k_0}\left\{\frac{\partial}{\partial R}\left(\frac{1}{R}\frac{\partial\overline{W}}{\partial\theta}\right)\right\}^2 + K_f\overline{W}^2 + \overline{N_r}\left(\frac{\partial\overline{W}}{\partial R}\right)^2$$
$$\left.+\overline{N_\theta}\left(\frac{1}{R}\frac{\partial\overline{W}}{\partial\theta}\right)^2\right]R\,\mathrm{d}\theta\,\mathrm{d}R + K_\phi\int_0^{2\pi}\left(\frac{\partial\overline{W}(1)}{\partial R}\right)^2\mathrm{d}\theta - \Omega^2\int_0^1\int_0^{2\pi}(1-\alpha R)\overline{W}^2R\,\mathrm{d}\theta\,\mathrm{d}R\Bigg], \tag{12}$$

where

$$D_{r_0} = \frac{E_r h_0^3}{12(1-\upsilon_r\upsilon_\theta)},\ D_{k_0} = \frac{D_k}{D_{r_0}},\ \Omega^2 = \frac{a^4\omega^2\rho h_0}{D_{r_0}},\ K_f = \frac{a^4k_f}{D_{r_0}},$$
$$K_\phi = \frac{ak_\phi}{D_{r_0}},\ \overline{N} = \frac{Na^2}{D_{r_0}},\ \overline{N_r} = \frac{N_ra^2}{D_{r_0}},\ \overline{N_\theta} = \frac{N_\theta a^2}{D_{r_0}}.$$

The minimization of the functional $J(\overline{W})$ given by (12) requires

$$\frac{\partial J(\overline{W})}{\partial A_i} = 0, \quad i = 0,1,2,\ldots,m. \tag{13}$$

This leads to a system of homogeneous equations in A_i, $i = 0,1,\ldots,m$, whose non-trivial solution leads to the frequency equation:

$$|A - \Omega^2 B| = 0, \tag{14}$$

where $A = [a_{ij}]$: and $B = [b_{ij}]$ are square matrices of order $m+1$ given by

$$a_{ij} = \int_0^1(1-\alpha R)^3\left[W_i''W_j'' + 2\upsilon_\theta W_i''\left(\frac{W_j'}{R}-n^2\frac{W_j}{R^2}\right) + p^2\left(\frac{W_i'}{R}-n^2\frac{W_i}{R^2}\right)\left(\frac{W_j'}{R}-n^2\frac{W_j}{R^2}\right)\right.$$
$$\left.+\,n^2D_{k_0}\left(\frac{W_j'}{R}-\frac{W_i}{R^2}\right)\left(\frac{W_j'}{R}-\frac{W_j}{R^2}\right) + K_fW_iW_j + \overline{N_r}W_i'W_j' + n^2\overline{N_\theta}W_{i-1}W_{j-1}\right]R\,\mathrm{d}R + K_\phi W_i'(1)W_j'(1) \tag{15}$$

and

$$b_{ij} = \int_0^1(1-\alpha R)W_iW_jR\,\mathrm{d}R. \tag{16}$$

4. Numerical results

The frequency equation (14) is solved by hybrid secant method retaining the advantages of certainty of bisection and the speed of the secant method. The equation has been solved for various values of plate parameters such as taper $\alpha(=0.0,\ \pm0.1,\ \pm0.3)$, rigidity ratio E_θ/E_r $(=0.75,\ 1.0,\ 5.0,\ 10.0)$, foundation parameter K_f $(=0.00\ (0.01)\ 0.05)$ and nodal diameter n $(=0,\ 1,\ 2)$ in presence of in-plane force parameter $\overline{N}$ $(=0,\ \pm5,\ \pm10)$. The Poisson's ratio υ_θ and shear modulus D_{k_0} has been fixed as 0.3 and 1.40, respectively. Special cases of boundary conditions: simply supported (SS) and clamped (CL) have been obtained by assigning $K_\Phi = 0.0$ and 10^{20}, respectively. The critical buckling load N_{cr} has been obtained for both the boundary conditions.

5. Discussion

Numerical results are presented in Tables 1–4 and Figs. 2–15 which show the effect of in-plane force parameter $\overline{N}$ and foundation parameter K_f on natural frequencies of vibrations for different values of taper parameter α and rigidity ratio p^2.

Table 1
Critical buckling load N_{cr} as a function of α and E_θ/E_r ($=p^2$) for SS plate in fundamental mode

α/p^2	$K_f = 0.01$					
	$n=0$		$n=1$		$n=2$	
	0.75	5.0	0.75	5.0	0.75	5.0
−0.3	22.6679	52.0044	26.7589	57.6830	42.1986	89.7517
−0.1	21.3607	41.6741	21.4068	42.1504	31.5585	62.0641
0.0	20.7716	37.1480	19.0750	35.6926	25.5393	50.7244
0.1	20.2157	32.9437	16.9572	30.0239	22.8741	40.8646
0.3	16.9207	25.0638	13.3023	20.7809	15.9671	25.2873
$K_f = 0.02$						
−0.3	39.4222	72.8375	33.6933	67.6066	46.1682	94.2062
−0.1	34.3916	60.0040	28.3333	51.5816	35.5567	66.3844
0.0	30.5526	53.8276	25.9858	44.8146	30.9865	54.9401
0.1	26.8309	47.6426	23.8376	38.7747	26.8755	44.9970
0.3	20.0615	34.9041	20.0017	28.4840	19.9135	29.1419

Table 2
Critical buckling load N_{cr} as a function of α and E_θ/E_r ($=p^2$) for a clamped plate in fundamental mode

α/p^2	$K_f = 0.01$					
	$n=0$		$n=1$		$n=2$	
	0.75	5.0	0.75	5.0	0.75	5.0
−0.3	30.8033	120.3900	43.1223	120.8408	62.2875	159.2562
−0.1	25.9509	90.0044	33.5066	86.1658	47.0144	110.7845
0.0	23.8465	77.2941	29.2772	71.7153	40.2987	90.6595
0.1	21.9355	66.0704	25.4236	59.0440	34.1897	73.0722
0.3	18.5574	47.4665	18.8141	38.5848	23.7078	44.8906
$K_f = 0.02$						
−0.3	40.3526	149.4571	48.1783	132.4250	65.4011	164.1939
−0.1	35.1995	117.3433	38.7260	97.3375	50.2463	115.5968
0.0	32.7675	103.5029	34.5808	82.6422	43.5928	95.3974
0.1	30.3314	90.8312	30.8129	69.6902	37.5482	77.7252
0.3	24.9996	67.2754	24.3726	48.5000	27.1967	49.3275

To choose the appropriate number of terms for the evaluation of frequency parameter Ω, a computer program was developed which was run for $m = 3(1)15$. Fig. 16 shows a consistent improvement in value of Ω with the increase in number of terms for specified plate parameters. The plots show that the present method has a faster rate of convergence as compared to polynomial coordinate functions employed in Ref. [37]. In all the computations we have fixed $m = 12$ since further increase in m does not improve the result except in the fourth or fifth place of decimal.

Table 1 gives critical buckling load parameter N_{cr} for SS plate for α ($= 0.0, \pm 0.1; \pm 0.3$), K_f ($= 0.01, 0.02$) and p^2 ($= 0.75, 5.0$). Results show that critical buckling load for radially stiffened plate ($p^2 < 1$) is less than that for corresponding circumferentially stiffened plate ($p^2 > 1$). Thus, the plates having reinforcement in circumferential direction have higher buckling resistance for axisymmetric ($n = 0$) as well as antisymmetric modes($n = 1, 2$). This is true whether the plate is centrally thick ($\alpha < 0$) or centrally thin ($\alpha > 0$) or is of uniform

Table 3
Frequency parameter Ω as a function of taper parameter α, in-plane force parameter $\overline{N}$ and rigidity ratio E_θ/E_r for a simply supported plate

p^2	$K_f = 0.01$				$K_f = 0.02$			
	0.75		5.00		0.75		5.00	
$\overline{N}/\alpha$	−0.30	0.30	−0.30	0.30	−0.30	0.30	−0.30	0.30
$n = 0$								
Ω_{00}								
−10.0	8.2340	8.0748	13.2756	11.0087	12.7099	13.6599	16.7281	16.1048
−5.0	9.7168	10.0398	13.9862	12.3242	13.7155	14.9029	17.2999	17.0101
0.0	10.9998	11.6758	14.6540	13.4338	14.6513	16.0496	17.8464	17.8149
5.0	12.1469	13.1084	15.2855	14.4072	15.5301	17.1195	18.3705	18.5481
10.0	13.1938	14.3987	15.8854	15.2838	16.3613	18.1263	18.8745	19.2275
Ω_{01}								
−10.0	30.1920	16.9525	45.6377	30.4954	31.7011	20.3261	46.7624	32.7330
−5.0	32.5457	22.1829	46.4010	32.5971	33.9501	24.8557	47.5077	34.7028
0.0	34.7347	26.3924	47.1493	34.5279	36.0536	28.6743	48.2389	36.5241
5.0	36.7887	30.0142	47.8833	36.3150	38.0361	32.0382	48.9568	38.2183
10.0	38.7298	33.2416	48.6036	37.9803	39.9163	35.0790	49.6617	39.8039
$n = 1$								
Ω_{10}								
−10.0	14.7883	7.9080	21.3820	13.3874	17.5915	13.7936	23.6196	17.9748
−5.0	16.8445	12.5199	22.4377	15.9972	19.3513	16.8603	24.5804	19.9820
0.0	18.6739	15.8313	23.4406	18.1611	20.9625	19.4427	25.5000	21.7432
5.0	20.3381	18.5560	24.3975	20.0389	22.4572	21.7167	26.3832	23.3266
10.0	21.8751	20.9260	25.3138	21.7152	23.8576	23.7721	27.2336	24.7749
Ω_{11}								
−10.0	52.2668	32.4153	64.8887	43.0045	53.1410	34.3160	65.6726	44.6281
−5.0	54.4274	37.1434	65.7551	45.3343	55.2674	38.8142	66.5286	46.8785
0.0	56.5031	41.3315	66.6085	47.5221	57.3126	42.8396	67.3722	48.9981
5.0	58.5030	45.1299	67.4494	49.5860	59.2851	46.5150	68.2037	51.0026
10.0	60.4348	48.6300	68.2784	51.5411	61.1921	49.9180	69.0236	52.9054
$n = 2$								
Ω_{20}								
−10.0	26.8729	14.0477	41.1344	23.6607	28.4861	18.1154	42.3208	26.6114
−5.0	28.8757	19.0270	42.3719	27.0917	30.3825	22.1973	43.5252	29.6974
0.0	30.7470	22.9415	43.5715	30.0794	32.1659	25.6300	44.6942	32.4407
5.0	32.5095	26.2738	44.7361	32.7525	33.8544	28.6497	45.8308	34.9288
10.0	34.1802	29.2250	45.8686	35.1884	35.4616	31.3772	46.9374	37.2181
Ω_{21}								
−10.0	76.4419	48.9736	99.7340	65.7854	77.0359	50.2665	100.3245	66.8432
−5.0	78.5005	53.4736	100.7190	68.3848	79.0790	54.6605	101.3049	69.3954
0.0	80.5051	57.6210	101.6935	70.8708	81.0692	58.7243	102.2750	71.8375
5.0	82.4596	61.4869	102.6578	73.2547	83.0105	62.5220	103.2351	74.1798
10.0	84.3677	65.1216	103.6122	75.5460	84.9062	66.0997	104.1853	76.4311

thickness ($\alpha = 0$). Further the buckling load N_{cr} is found to increase with the increase in foundation parameter K_f, keeping all other parameters fixed.

Table 2 gives buckling load N_{cr} for a CL plate. The value of N_{cr} is found to increase with the increase in foundation parameter K_f similar to SS plate. The buckling load for a plate with CL edge is found to be always greater than that for the corresponding SS plate.

Table 4
Frequency parameter Ω as a function of taper parameter α, in-plane force parameter $\overline{N}$ and rigidity ratio E_θ/E_r for a clamped plate

p^2	$K_f = 0.01$				$K_f = 0.02$			
	0.75		5.00		0.75		5.00	
$\overline{N}/\alpha$	−0.30	0.30	−0.30	0.30	−0.30	0.30	−0.30	0.30
$n = 0$								
Ω_{00}								
−10.0	13.0641	9.3865	19.4428	14.0424	16.3329	14.3462	21.9952	18.2105
−5.0	14.4064	11.5043	19.8648	14.8771	17.4210	15.8311	22.3695	18.8578
0.0	15.6040	13.2151	20.2773	15.6579	18.4204	17.1259	22.7369	19.4763
5.0	16.6933	14.6899	20.6807	16.3936	19.3490	18.2953	23.0977	20.0696
10.0	17.6981	16.0062	21.0756	17.0908	20.2199	19.3735	23.4522	20.6405
Ω_{01}								
−10.0	42.5485	26.1006	59.4974	40.2311	43.6309	28.3932	60.3370	41.9673
−5.0	44.5383	29.9792	60.0274	41.5812	45.5742	31.9888	60.8588	43.2675
0.0	46.4370	33.4189	60.5517	42.8732	47.4321	35.2295	61.3751	44.5157
5.0	48.2548	36.5358	61.0703	44.1132	49.2136	38.1970	61.8859	45.7174
10.0	50.0002	39.4037	61.5835	45.3061	50.9265	40.9476	62.3915	46.8777
$n = 1$								
Ω_{10}								
−10.0	23.8517	13.7283	30.9886	19.6543	25.7223	17.6780	32.6035	22.9417
−5.0	25.5035	17.1236	31.6697	21.2509	27.2596	20.4321	33.2518	24.3208
0.0	27.0403	19.9226	32.3359	22.7247	28.7013	22.8327	33.8870	25.6163
5.0	28.4822	22.3558	32.9879	24.0992	30.0626	24.9868	34.5099	26.8411
10.0	29.8440	24.5356	33.6267	25.3914	31.3551	26.9567	35.1211	28.0052
Ω_{11}								
−10.0	67.3209	43.3206	80.8398	54.3483	68.0045	44.7521	81.4731	55.6330
−5.0	69.2351	47.1328	81.4936	55.9922	69.9000	48.4504	82.1220	57.2396
0.0	71.0947	50.6580	82.1414	57.5765	71.7425	51.8853	82.7649	58.7900
5.0	72.9038	53.9515	82.7832	59.1067	73.5357	55.1048	83.4019	60.2890
10.0	74.6660	57.0529	83.4192	60.5873	75.2831	58.1442	84.0333	61.7409
$n = 2$								
Ω_{20}								
−10.0	38.1567	22.1809	54.5764	33.3530	39.3308	24.8895	55.4798	35.4564
−5.0	39.8683	25.8741	55.4728	35.6069	40.9929	28.2324	56.3617	37.5827
0.0	41.5012	29.0888	56.3544	37.7162	42.5822	31.2066	57.2295	39.5854
5.0	43.0650	31.9714	57.2219	39.7046	44.1072	33.9108	58.0838	41.4828
10.0	44.5672	34.6062	58.0759	41.5900	45.5747	36.4065	58.9253	43.2895
Ω_{21}								
−10.0	93.7527	61.3968	118.9642	79.4764	94.2400	62.4256	119.3228	80.3460
−5.0	95.6260	65.186a9	119.7642	81.4707	96.1039	66.1564	120.1192	82.3169
0.0	97.4614	68.7664	120.5582	83.4078	97.9303	69.6857	120.9097	84.2319
5.0	99.2608	72.1665	121.3464	85.2917	99.7213	73.0427	121.6945	86.0951
10.0	101.0262	75.4113	122.1290	87.1262	101.4787	76.2500	122.4736	87.9102

Tables 3 and 4 give the frequency parameter Ω for different values of taper constant α, in-plane force parameter $\overline{N}$, foundation parameter K_f and rigidity ratio p^2 for the first three modes of vibration for SS and CL plates, respectively. The frequency parameter Ω is found to increase with the increase in in-plane force parameter $\overline{N}$, rigidity ratio p^2 and foundation parameter K_f, keeping other parameters fixed. Results (Table 4) show that the behavior of frequency parameter Ω for a CL plate are similar to those for a SS plate.

Fig. 2 shows the plots for radial stress resultant N_r/N versus radius R for rigidity ratio ($p^2 = 10$, 1 and 0.1) for three values of taper constant α ($= 0.0$ and ± 0.3). The radial stress resultant remains constant for

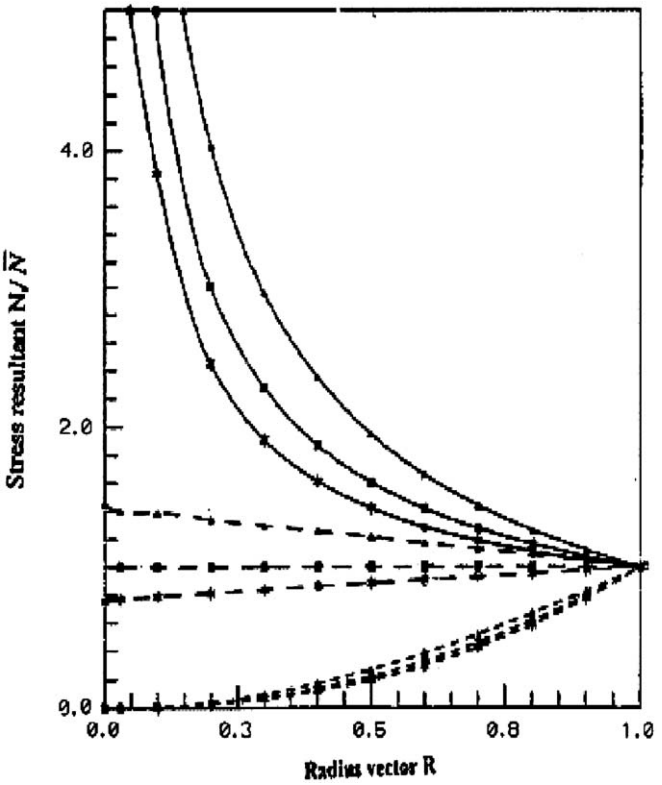

Fig. 2. Stress resultant for $p^2 = 10.0$: -----, $P^2 = 1.00$: – – – – – and $p^2 = 0.10$: —— $\alpha = -0.3$: ∗-∗-∗, $\alpha = 0.0$: ■-■-■ and $\alpha = 0.3$: ▲-▲-▲.

isotropic plate of uniform thickness. For circumferentially stiffened plates it is found to decrease, while for radially stiffened plates, it is found to increase from center to the edge. The plots show that for small values of p^2 instability arises near center. The stress resultant N_r for circumferentially stiffened plates remains greater than the applied load N while it is just the reverse for radially stiffened plates.

Fig. 3 presents the graph for Ω versus compressive in-plane force parameter $\overline{N}$ (i.e. $\overline{N}<0$) for SS and CL plates. The frequency parameter Ω is found to increase as the in-plane force parameter $\overline{N}$ increases for both types of plates. Figs. 4 and 5 present the plots for Ω versus K_f in axisymmetric mode of vibration for $\overline{N}$ (= 0, 10) for taper constant $\alpha = \pm 0.3$ for a SS plate for p^2 (= 0.75, 1.0, 10.0). The graphs show that the rate of increase of Ω with increase in K_f for $\overline{N} = 0.0$ is greater than that for $\overline{N} = 10$ in the range of foundation parameter values considered. Further, the rate of increase of Ω for radially stiffened plate is greater than that for circumferentially stiffened plate. The rate of increase of Ω for $\alpha = -0.3$ is greater than that for $\alpha = 0.3$ with increasing values of K_f. Figs. 6 and 7 show the behavior of Ω with increasing values of K_f (in case of antisymmetric mode $n = 1$) for taper constant $\alpha = \pm 0.3$. The plots in Figs. 8 and 9 for antisymmetric mode $n = 2$ show that Ω increases almost linearly with increasing K_f for both types of thickness variations ($\alpha = \pm 0.3$). Figs. 10–15 present plots of Ω versus K_f for a CL plate for all the three modes of vibration. Results show that the frequency parameter Ω for a CL plate are greater than that for SS plate for respective values of plate parameters. The effect of elastic foundation is found to be increasingly pronounced with the increasing modes (Figs. 12–15) for centrally thick ($\alpha = -0.3$) plates as compared to the corresponding centrally thin ($\alpha = 0.3$) plates for $\overline{N} = 10$.

A comparison of our results regarding critical buckling load N_{cr} for isotropic plates with those of Pardoen [38] obtained by finite element technique and the exact values of Volmir [39] is given in Table 5. The comparison of the values of N_{cr} for tapered polar orthotropic plates by Bhushan et al. [7] employing semi-analytic finite element technique in which geometric stiffness matrix is constructed by using radial stress

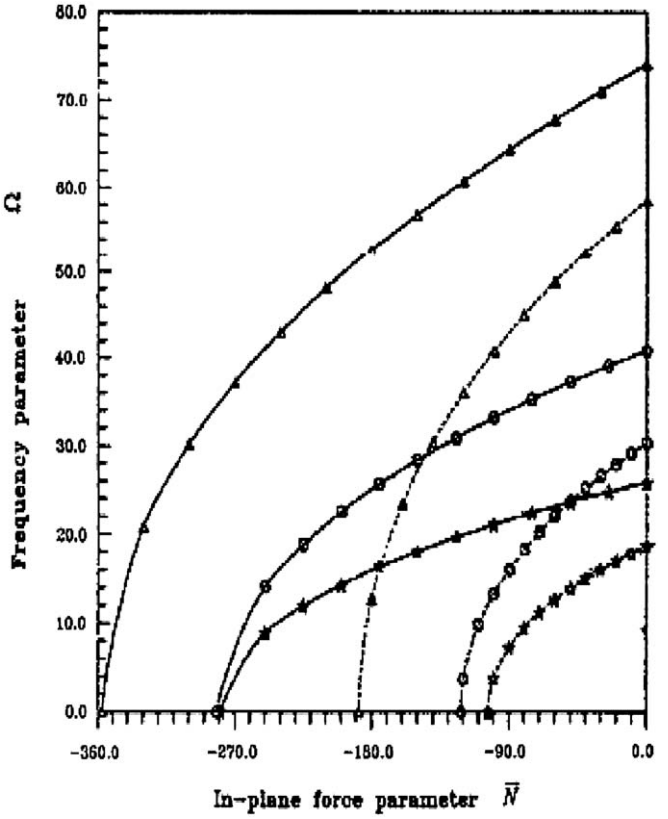

Fig. 3. Fundamental frequency for SS: ----- and Cl: —— for $n = 0$: ∗-∗-∗, $n = 1$: ○-○-○ and $n = 2$: △-△-△.

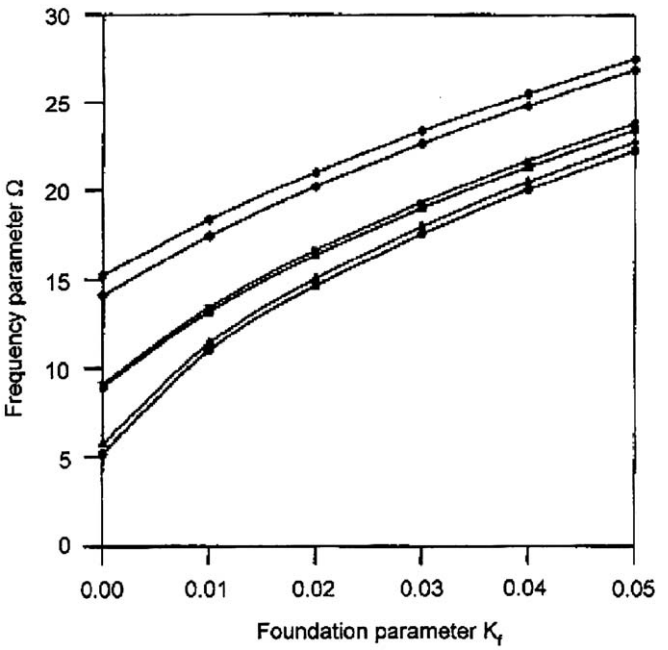

Fig. 4. Fundamental frequency parameter Ω for SS plate in axisymmetric mode ($n = 0$) for taper parameter $\alpha = -0.3\, p^2 = 0.75$; $\overline{N} = 0.0$: ●-●-●; $\overline{N} = 10$: ■-■-■, $p^2 = 1.00$; $\overline{N} = 0.0$: ▲-▲-▲; $\overline{N} = 10$: ▼-▼-▼ and $p^2 = 10.00$; $\overline{N} = 0.0$: ◆-◆-◆; $\overline{N} = 10$: ⬢-⬢-⬢.

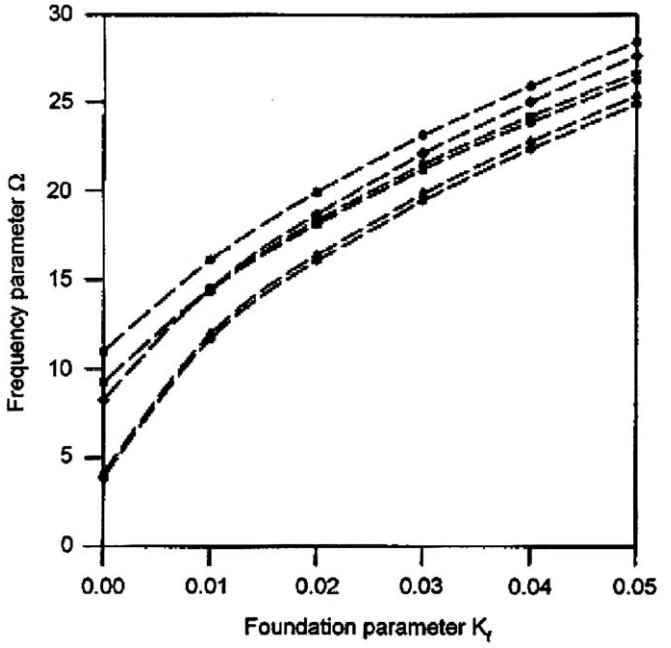

Fig. 5. Fundamental frequency parameter Ω for SS plate in axisymmetric mode ($n = 0$) for taper parameter $\alpha = -0.3$ $p^2 = 0.75$; $\overline{N} = 0.0$: ● ● ●; $\overline{N} = 10$: ■-■-■, $p^2 = 1.00$; $\overline{N} = 0.0$: ▲-▲-▲; $\overline{N} = 10$: ▼-▼-▼ and $p^2 = 10.00$; $\overline{N} = 0.0$: ◆-◆-◆; $\overline{N} = 10$: ⬢-⬢-⬢.

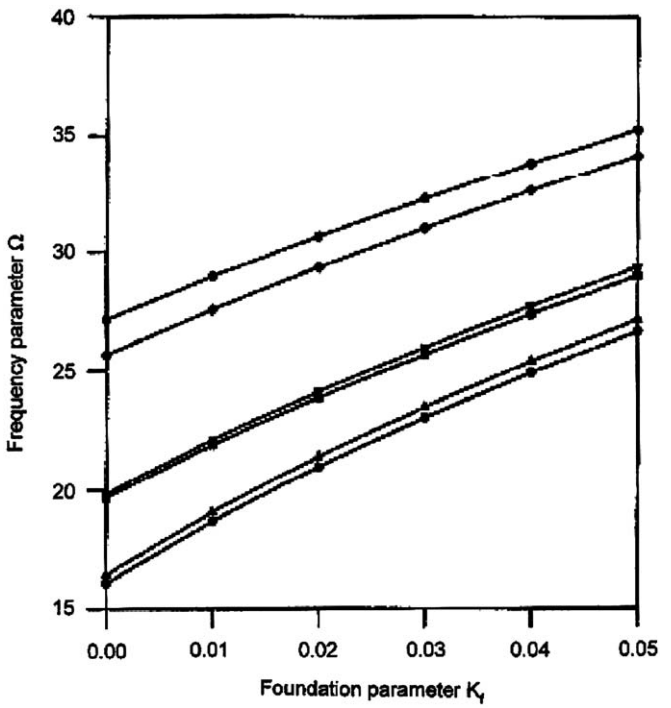

Fig. 6. Fundamental frequency parameter Ω SS plate in axisymmetric mode ($n = 1$) for taper parameter $\alpha = -0.3\, p^2 = 0.75$; $\overline{N} = 0.0$: ●-●-●; $\overline{N} = 10$: ■-■-■, $p^2 = 1.00$; $\overline{N} = 0.0$: ▲-▲-▲; $\overline{N} = 10$: ▼-▼-▼ and $p^2 = 10.00$; $\overline{N} = 0.0$: ◆-◆-◆; $\overline{N} = 10$: ⬢-⬢-⬢.

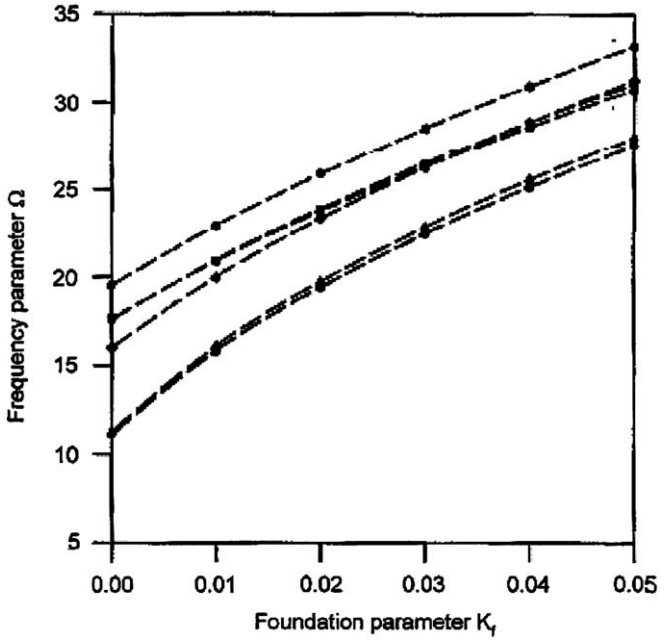

Fig. 7. Fundamental frequency parameter Ω for SS plate in antisymmetric mode ($n = 1$) for taper parameter $\alpha = -0.3\, p^2 = 0.75$; $\overline{N} = 0.0$: ●-●-●; $\overline{N} = 10$: ■-■-■, $p^2 = 1.00$; $\overline{N} = 0.0$: ▲-▲-▲; $\overline{N} = 10$: ▼-▼-▼ and $p^2 = 10.00$; $\overline{N} = 0.0$: ◆-◆-◆; $\overline{N} = 10$: ⬢-⬢-⬢.

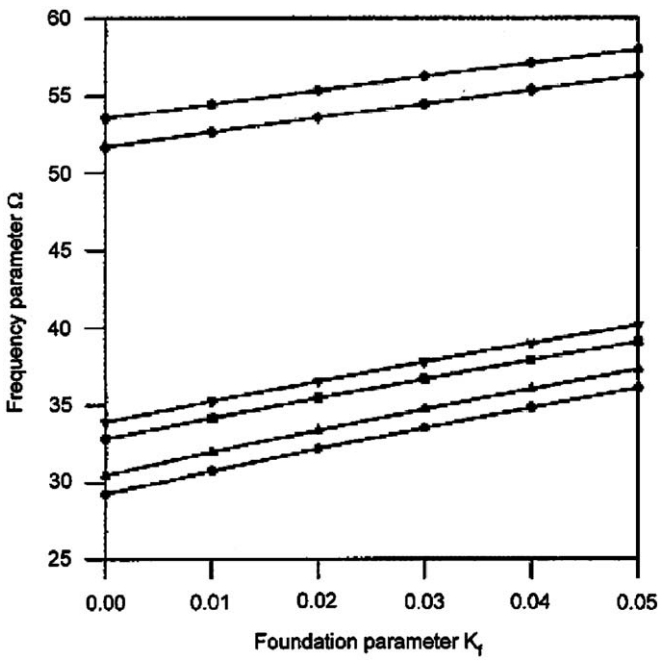

Fig. 8. Fundamental frequency parameter Ω for SS plate in antisymmetric mode ($n = 2$) for taper parameter $\alpha = -0.3\, p^2 = 0.75$; $\overline{N} = 0.0$: ●-●-●; $\overline{N} = 10$: ■-■-■, $p^2 = 1.00$; $\overline{N} = 0.0$: ▲-▲-▲; $\overline{N} = 10$: ▼-▼-▼ and $p^2 = 10.00$; $\overline{N} = 0.0$: ◆-◆-◆; $\overline{N} = 10$: ⬢-⬢-⬢.

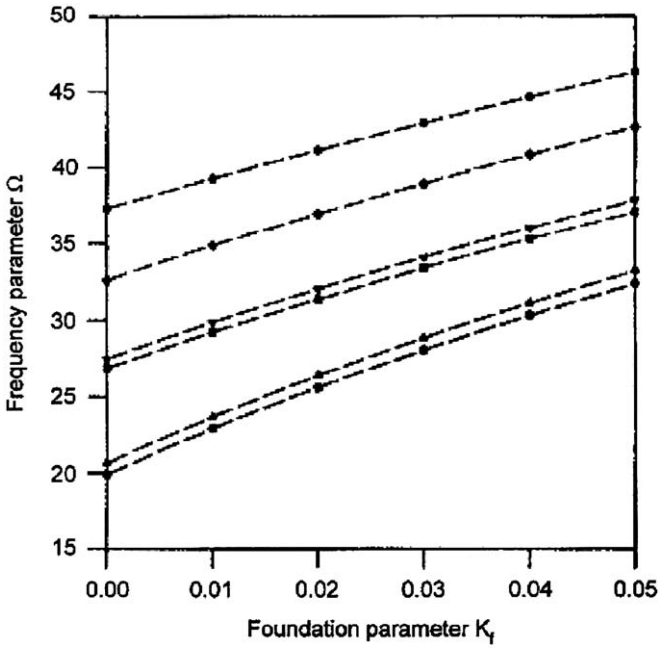

Fig. 9. Fundamental frequency parameter Ω for SS plate in antisymmetric mode ($n = 2$) for taper parameter $\alpha = -0.3$ $p^2 = 0.75$; $\bar{N} = 0.0$: ●-●-●; $\overline{N} = 10$: ■-■-■, $p^2 = 1.00$; $\overline{N} = 0.0$: ▲-▲-▲; $\overline{N} = 10$: ▼-▼-▼ and $p^2 = 10.00$; $\overline{N} = 0.0$: ◆-◆-◆; $\overline{N} = 10$: ⬢-⬢-⬢.

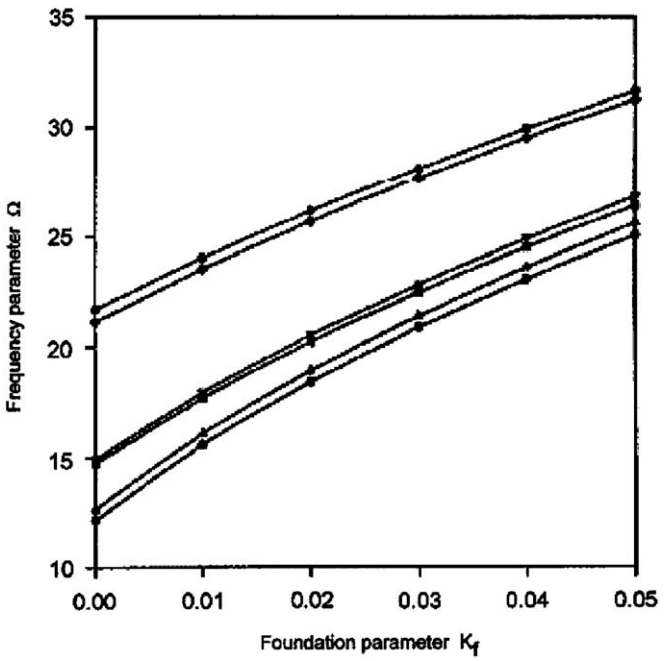

Fig. 10. Fundamental frequency parameter Ω for CL plate in antisymmetric mode ($n = 0$) for taper parameter $\alpha = -0.3$ $p^2 = 0.75$; $\overline{N} = 0.0$: ●-●-●; $\overline{N} = 10$: ■-■-■, $p^2 = 1.00$; $\overline{N} = 0.0$: ▲-▲-▲; $\overline{N} = 10$: ▼-▼-▼ and $p^2 = 10.00$; $\overline{N} = 0.0$: ◆-◆-◆; $\overline{N} = 10$: ⬢-⬢-⬢.

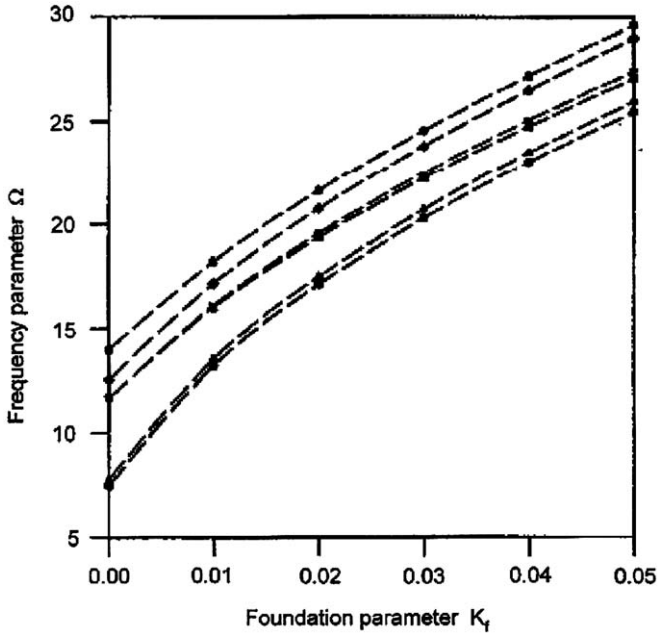

Fig. 11. Fundamental frequency parameter Ω for CL plate in axisymmetric mode ($n = 0$) for taper parameter $\alpha = -0.3\,p^2 = 0.75$; $\overline{N} = 0.0$: ●-●-●; $\overline{N} = 10$: ■-■-■, $p^2 = 1.00$; $\overline{N} = 0.0$: ▲-▲-▲; $\overline{N} = 10$: ▼-▼-▼ and $p^2 = 10.00$; $\overline{N} = 0.0$: ◆-◆-◆; $\overline{N} = 10$: ⬢-⬢-⬢.

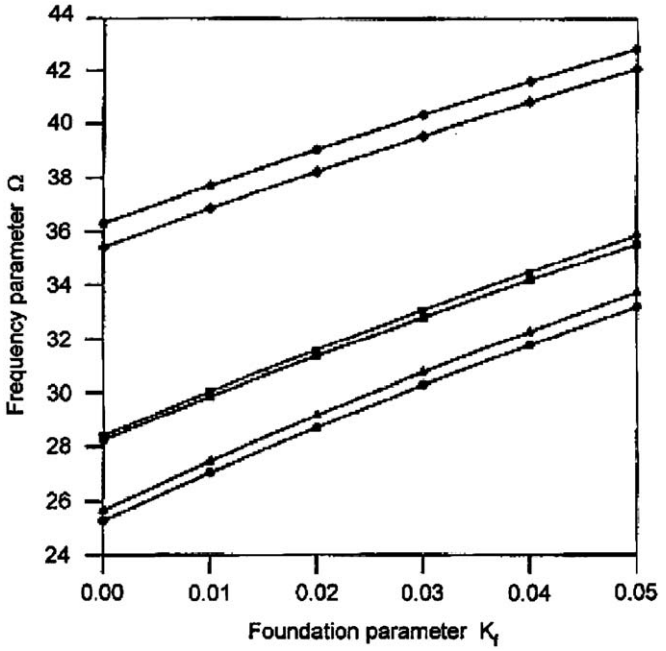

Fig. 12. Fundamental frequency parameter Ω for CL plate in axisymmetric mode ($n = 1$) for taper parameter $\alpha = -0.3\,p^2 = 0.75$; $\overline{N} = 0.0$: ●-●-●; $\overline{N} = 10$: ■-■-■, $p^2 = 1.00$; $\overline{N} = 0.0$: ▲-▲-▲; $\overline{N} = 10$: ▼-▼-▼ and $p^2 = 10.00$; $\overline{N} = 0.0$: ◆-◆-◆; $\overline{N} = 10$: ⬢-⬢-⬢.

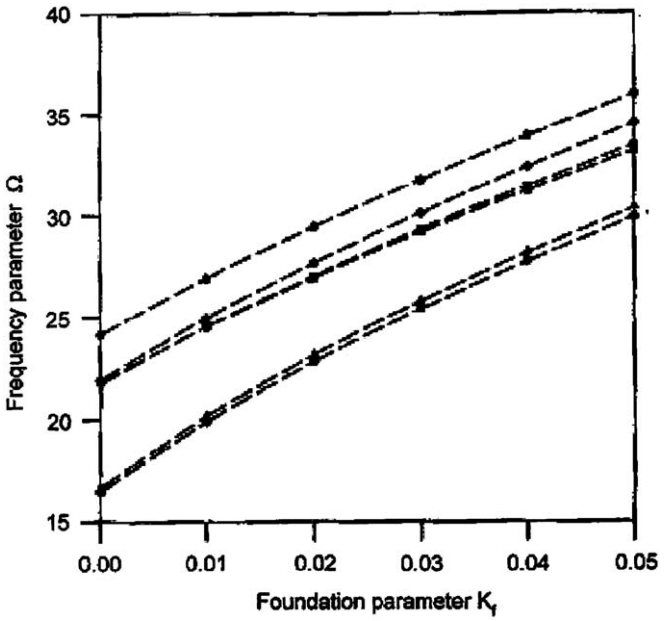

Fig. 13. Fundamental frequency parameter Ω for CL plate in antisymmetric mode ($n = 1$) for taper parameter $\alpha = -0.3$ $p^2 = 0.75$; $\overline{N} = 0.0$: ●-●-●; $\overline{N} = 10$: ■-■-■, $p^2 = 1.00$; $\overline{N} = 0.0$: ▲-▲-▲; $\overline{N} = 10$: ▼-▼-▼ and $p^2 = 10.00$; $\overline{N} = 0.0$: ◆-◆-◆; $\overline{N} = 10$: ⬢-⬢-⬢.

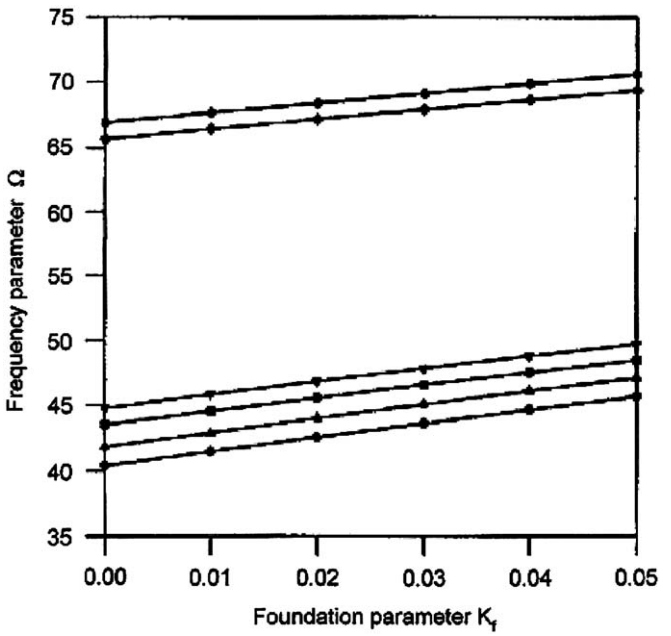

Fig. 14. Fundamental frequency parameter Ω for CL plate in antisymmetric mode ($n = 2$) for taper parameter $\alpha = -0.3$ $p^2 = 0.75$; $\overline{N} = 0.0$: ●-●-●; $\overline{N} = 10$: ■-■-■, $p^2 = 1.00$; $\overline{N} = 0.0$: ▲-▲-▲; $\overline{N} = 10$: ▼-▼-▼ and $p^2 = 10.00$; $\overline{N} = 0.0$: ◆-◆-◆; $\overline{N} = 10$: ⬢-⬢-⬢.

distribution rather than computationally expensive finite element stress analysis is given in Table 6. A comparison of results for N_{cr} for different values of flexibility parameter K_Φ and taper parameter α for isotropic plates by Gutierrez et al. [40] using differential quadrature method is given in Table 7. Table 8 gives comparison of values of natural frequency parameter Ω for isotropic circular plates of linearly varying

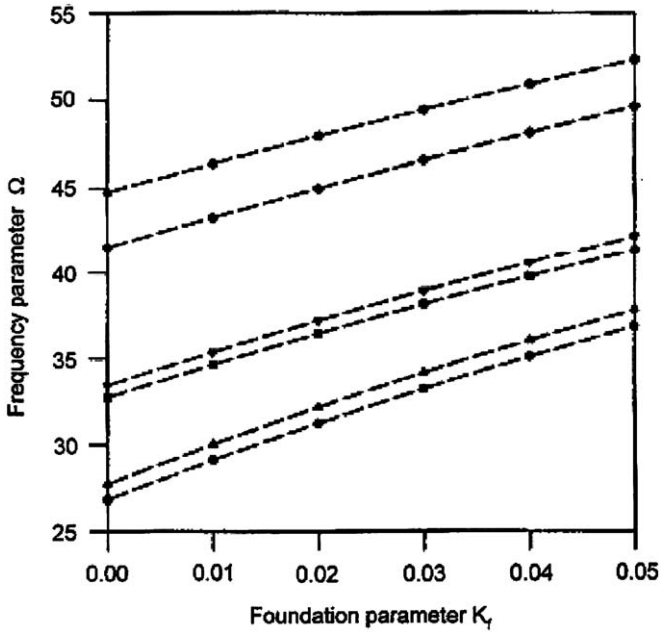

Fig. 15. CL plate for taper $\alpha = 0.3$ in antisymmetric mode ($n = 2$). Fundamental frequency parameter Ω for CL plate in antisymmetric mode ($n = 2$) for taper parameter $\alpha = -0.3\, p^2 = 0.75$; $\overline{N} = 0.0$: ●-●-●; $\overline{N} = 10$: ■-■-■, $p^2 = 1.00$; $\overline{N} = 10$: ▲-▲-▲; $\overline{N} = 10$: ▼-▼-▼ and $p^2 = 10.00$; $\overline{N} = 0.0$: ◆-◆-◆; $\overline{N} = 10$: ⬢-⬢-⬢.

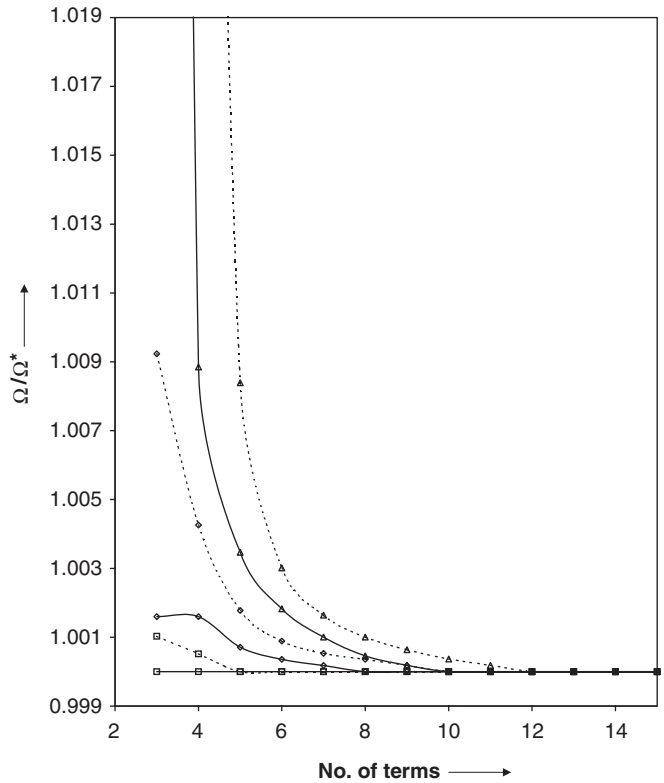

Fig. 16. Convergence of normalized frequency parameter, Ω/Ω^*, with no of terms used for the first three natural frequencies for $K_\Phi = 10^{20}$, $E_\theta/E_r = 5.0$, $n = 1$, $\alpha = 0.3$. —, present method; ----, polynomial coordinate method. □, Fundamental mode; ◇, second mode; △, third mode Ω^*-the frequency using 15 terms.

Table 5
Comparison of critical buckling load parameter N_{cr} of isotropic plates with those obtained by finite element method and with exact solution

$n=0$			$n=1$			$n=2$		
f.e.m.	Exact	Present	f.e.m.	Exact	Present	f.e.m.	Exact	Present
SS								
4.1978	4.1978	4.1978	13.1385	13.1381	13.1381	24.8579	24.8557	24.8557
29.0495	29.0452	29.0452	47.7966	47.7814	47.7814	69.4554	69.4097	69.4097
73.5495	73.4768	73.4768	102.2246	102.0823	102.0823	133.9121	133.6001	133.6001
Cl								
14.6825	14.6820	14.6820	26.3772	26.3746	26.3746	40.7156	40.7064	40.7064
49.2394	49.2185	49.2185	70.8974	70.8499	70.8499	95.3910	95.2775	95.2775
103.4995	103.4995	103.4995	135.3394	135.0207	135.0207	170.0098	169.3954	169.3954

f.e.m.: values taken from Ref. [38], exact: values taken from Ref. [39].

Table 6
Comparison of critical buckling load parameter N_{cr} of tapered orthotropic plates

α/p^2	SS-plate				Cl-plate			
	f.e.m.		Present		f.e.m.		Present	
	1	10	1	10	1	10	1	10
−0.5	3.5873	10.4851	3.5873	10.4847	13.5154	32.3417	13.5154	32.3295
−0.3	3.7875	10.0005	3.7875	10.0001	13.9774	30.9003	13.9770	30.8872
0.0	4.1978	9.0693	4.1978	9.0685	14.6824	27.9817	14.6820	27.9670
0.3	4.8014	7.7574	4.8014	7.7556	15.2363	23.5980	15.2357	23.5822
0.5	5.3272	6.7330	5.3270	6.5294	15.2202	19.3163	15.2194	19.3012

f.e.m.: values taken from Ref. [7].

Table 7
Comparison of critical buckling load parameter N_{cr} as a function of the rotational flexibility coefficient and the taper parameter α in fundamental mode

α/K_ϕ	Present					From Ref. [40]				
	0	1	10	50	∞	0	1	10	50	∞
−0.3	2.4583	4.4587	7.1460	7.6613	7.8007	2.504	4.561	7.363	7.907	8.054
−0.1	3.5561	5.6863	10.4222	11.7387	12.1143	3.577	5.725	10.522	11.861	12.243
0.0	4.1978	6.3532	12.1725	14.1106	14.6820	4.198	6.353	12.173	14.111	14.682
0.1	4.9070	7.0733	13.9679	16.7020	17.5375	4.879	7.029	13.844	16.535	17.537
0.3	6.5448	8.5448	17.6255	22.5150	24.1521	6.438	8.556	17.196	21.873	23.432

thickness and resting on elastic foundation with those of Laura et al. [37] using polynomial coordinate function. The comparison of results shows that, our results are in good agreement with those available in literature. In Ritz method, the choice of functions to approximate the deflection plays an important role. The present choice of basis functions based upon the static deflection for polar orthotropic plates (Lekhnitskii [36, p. 370]) is found to have a faster rate of convergence as compared to the choice of polynomial coordinate functions and is given in Table 9.

Table 8
Comparison of frequency parameter Ω for simply supported isotropic circular plate of linearly varying thickness resting on elastic foundation for first two modes; $v_\theta = 0.33$

α/Ω	Ω_{00}	Ω_{01}	Ω_{10}	Ω_{11}	Ω_{20}	Ω_{21}
$K_f = 10$						
−0.2	6.2992	33.1186	15.9140	53.8956	29.0618	78.1215
	6.30[a]	33.12[a]	15.91[a]	53.93[a]	29.06[a]	78.35[a]
−0.1	6.0947	31.5258	15.1015	51.2711	27.4543	74.1936
	6.10[a]	31.53[a]	15.10[a]	51.29[a]	27.46[a]	74.29[a]
0.0	5.8983	29.9220	14.2899	48.6153	25.8429	70.2211
	5.90[a]	29.94[a]	14.29[a]	48.63[a]	25.85[a]	70.26[a]
0.1	5.7111	28.3050	13.4755	45.9231	24.2269	66.1965
	5.72[a]	28.35[a]	13.48[a]	45.95[a]	24.23[a]	66.22[a]
0.2	5.5342	26.6718	12.6580	43.1880	22.6058	62.1101
	5.54[a]	26.74[a]	12.66[a]	43.26[a]	22.61[a]	62.15[a]
$K_f = 20$						
−0.2	12.5988	44.6540	24.5677	67.9236	39.7539	94.4479
	12.62[a]	44.69[a]	24.58[a]	68.13[a]	39.76[a]	95.33[a]
−0.1	11.8681	42.3497	23.1497	64.4819	37.4650	89.6064
	11.89[a]	42.38[a]	23.16[a]	64.58[a]	37.47[a]	90.10[a]
0.0	11.1518	40.0218	21.7257	60.9928	35.1626	84.7008
	11.18[a]	40.06[a]	21.74[a]	61.58[a]	35.17[a]	84.94[a]
0.1	10.4532	37.6663	20.2954	57.3569	32.6830	79.6540
	10.48[a]	37.74[a]	20.31[a]	57.49[a]	32.86[a]	79.83[a]
0.2	9.7762	35.2782	18.8590	53.8397	30.5092	74.6511
	9.80[a]	35.42[a]	18.87[a]	53.92[a]	30.52[a]	74.72[a]

[a]Values are taken from Ref. [37].

Table 9
Comparison of frequency parameter Ω obtained by using polynomial co-ordinate function and present method for $E_\theta/E_r = 10.0$ and $\alpha = -0.5$ and$v_\theta = 0.3$ in fundamental mode

	SS-plate			CL-plate		
	$n = 0$	$n = 1$	$n = 2$	$n = 0$	$n = 1$	$n = 2$
Frequency parameter Ω	78.5907	110.6255	183.7395	242.3338	266.8726	351.3450
No. of terms in present method	6	6	8	8	6	10
No. of terms in polynomial coordinate function	8	9	10	10	11	13

6. Conclusion

The paper presents results for natural frequencies and buckling loads for circular plates incorporating complicating effects such as polar orthotropy, thickness variation, elastic force and elastically restrained edge. Numerical results show that the presence of elastic foundation increases the frequency parameter for CL as well as SS plates. The critical buckling load parameter also gets increased due to elastic foundation whatever are other plate parameters. A desired frequency can be obtained by a proper choice of plate parameters.

References

[1] A.W. Leissa, *Vibration of plates*, NASA, SP-160, 1969.
[2] A.W. Leissa, Recent studies in plate vibrations 1981–1985, part-II: complicating effects, *The Shock and Vibration Digest* 19 (3) (1987) 10–24.

[3] G.K. Ramaiah, V. Kumar, Natural frequencies of polar orthotropic annular plates, *Journal of Sound and Vibration* 26 (4) (1973) 517–531.
[4] C.T. Dyka, J.F. Carney III, Vibration and stability of spinning polar orthotropic annular plates reinforced with edge beams, *Journal of Sound and Vibration* 64 (2) (1979) 223–231.
[5] D.G. Gunaratnam, A.P. Bhattacharya, Transverse vibration and stability of polar orthotropic circular plates: high level relationship, *Journal of Sound and Vibration* 137 (1989) 383–392.
[6] C.S. Kim, S.M. Dickinson, The flexural vibration of thin isotropic and polar orthotropic annular and circular plates with elastically restrained peripheries, *Journal of Sound and Vibration* 143 (1990) 171–179.
[7] B. Bhushan, G. Singh, G.V. Rao, Buckling of tapered orthotropic circular plates using a computationally economic approach, *Computers & Structures* 46 (3) (1993) 421–428.
[8] C.F. Liu, G.T. Chen, A simple finite element analysis of axisymmetric vibration of annular and circular plates, *International Journal of Mechanical Sciences* 37 (8) (1995) 861–871.
[9] B. Bhushan, G. Singh, G.V. Rao, Asymmetric buckling of layered orthotropic circular and annular plates of varying thickness using a computationally economic semi analytic finite element approach, *Computers & Structures* 59 (1) (1996) 21–33.
[10] U.S. Gupta, A.H. Ansari, Free vibration of polar orthotropic circular plates of variable thickness with elastically restrained edge, *Journal of Sound and Vibration* 213 (3) (1998) 429–445.
[11] U.S. Gupta, A.H. Ansari, Asymmetric vibration and elastic stability of polar orthotropic circular plate of linearly varying profile, *Journal of Sound and Vibration* 215 (2) (1998) 123–150.
[12] R. Szilard, *Theory and Analysis of Plates*, Prentice-Hall, Englewood Cliffs, NJ, 1974.
[13] S. Chonan, Random vibration of an initially stressed thick plate on an elastic foundation, *Journal of Sound and Vibration* 71 (1980) 117–127.
[14] U.S. Gupta, R. Lal, S.K. Jain, Effect of elastic foundation on axisymmetric vibration of polar orthotropic circular plates of variable thickness, *Journal of Sound and Vibration* 139 (3) (1990) 503–513.
[15] K.M. Liew, J.B. Han, M. Xiao, H. Do, Differential quadrature method for Mindlin plates on Winkler foundation, *International Journal of Mechanical Sciences* 38 (4) (1996) 405–421.
[16] T.M. Wang, J.E. Stephens, Natural frequencies of Timoshenko beams on pasternak foundation, *Journal of Sound and Vibration* 51 (1977) 149–155.
[17] B. Bhattacharya, Free vibration of plates on Vlasov's foundation, *Journal of Sound and Vibration* 54 (1977) 464–467.
[18] U.S. Gupta, R. Lal, C.P. Verma, Buckling and vibration of polar orthotropic annular plates on an elastic foundation subjected to hydrostatic peripheral loading, *Journal of Sound and Vibration* 109 (3) (1986) 423–434.
[19] J.B. Greenberg, Y. Stavsky, Flexural vibrations of certain full and annular composite orthotropic plates, *Journal of the Acoustical Society of America* 66 (1979) 501–508.
[20] D.Y. Chen, B.S. Ren, Finite element analysis of the lateral vibration of thin annular and circular plates with variable thickness, *ASME Journal of Vibration and Acoustics* 120 (3) (1998) 747–752.
[21] C.F. Liu, Y.T. Lee, Finite element analysis of three dimensional vibrations of thick circular and annular plates, *Journal of Sound and Vibration* 233 (1) (2000) 63–80.
[22] E. Charbonneau, A.A. Lakis, Semi-analytical shape functions in the finite element analysis of rectangular plates, *Journal of Sound and Vibration* 242 (3) (2001) 427–444.
[23] W. Ritz, Uber eine neue methode zur losung geuisser variations probleme der mathematischen physik, *Journal fur Reine und Angewandte Mathematic* 135 (1909) 1–61.
[24] K.M. Liew, Y. Xiang, S. Kitipornchai, Research on thick plate vibration: a literature survey, *Journal of Sound and Vibration* 180 (1) (1995) 163–176.
[25] R.B. Bhat, Natural frequencies of rectangular plates using characteristic orthogonal polynomials in Rayleigh–Ritz method, *Journal of Sound and Vibration* 102 (1985) 493–499.
[26] R.B. Bhat, Flexural vibration of polygonal plates using characteristic orthogonal polynomials in two variables, *Journal of Sound and Vibration* 114 (1987) 65–71.
[27] S.M. Dickinson, A.D. Blasio, On the use of orthogonal polynomials in the Rayleigh–Ritz method for the study of the flexural vibration and buckling of isotropic and orthotropic rectangular plates, *Journal of Sound and Vibration* 108 (1986) 51–62.
[28] K.M. Liew, K.Y. Lam, S.T. Chow, Study on flexural vibration of triangular composite plates influenced by fibre orientation, *Composite Structures* 13 (1989) 123–132.
[29] K.M. Liew, K.Y. Lam, S.T. Chow, Free vibration analysis of rectangular plates influenced by fiber orientation, *Computers & Structures* 34 (1990) 79–85.
[30] K.M. Liew, K.Y. Lam, Application of two-dimensional orthogonal plate function to flexural vibration of skew plates, *Journal of Sound and Vibration* 139 (2) (1990) 241–252.
[31] K.M. Liew, Vibration of clamped circular symmetric laminates, *Journal of Vibration and Acoustics* 116 (1994) 141–145.
[32] D. Zhou, Y.K. Cheung, F.T.K. Au, S.H. Lo, Three dimensional vibration analysis of thick rectangular plates using Chebyshev polynomials and Ritz method, *International Journal of Solids and Structures* 39 (2002) 6339–6353.
[33] D. Zhou, F.T.K. Au, Y.K. Cheung, S.H. Lo, Three dimensional vibration analysis of circular and annular plates via the Chebyshev–Ritz method, *International Journal of Solids and Structures* 40 (12) (2003) 3089–3105.
[34] J.H. Kang, Three dimensional vibration analysis of thick circular and annular plates with non-linear thickness variation, *Computers & Structures* 81 (2003) 1663–1675.

[35] W. Kang, N.H. Lee, S. Pang, W.Y. Chang, Approximate closed form solutions for free vibration of polar orthotropic circular plates, *Applied Acoustics* 66 (2005) 1162–1179.
[36] S.G. Lekhnitskii, *Anisotropic Plates*, Breach Science Publishers Inc., New York, 1985.
[37] P.A.A. Laura, R.H. Gutierrez, Free vibration of a solid circular plate of linearly varying thickness and attached to a Winkler type foundation, *Journal of Sound and Vibration* 144 (1) (1991) 149–167.
[38] G.C. Pardoen, Asymmetric vibration and stability of circular plates, *Computers & Structures* 9 (1978) 89–95.
[39] A.S. Volmir, *Stability of elastic system*, FTD-Mt-64-335, Wp-AFB, Ohio, 1966.
[40] R.H. Gutierrez, E. Romanelli, P.A.A. Laura, Vibration and elastic stability of thin circular plates with variable profile, *Journal of Sound and Vibration* 195 (3) (1996) 391–399.